Electronic Supplementary Material (ESI) for Journal of Materials Chemistry C.
This journal is © The Royal Society of Chemistry 2021

Supporting Info: Anisotropic silica colloids for light scattering

Gianni Jacucci[#,1,a], Brooke W. Longbottom[1,a,b], Christopher C. Parkins[a,b], Stefan A. F. Bon[b] and Silvia Vignolini[a]

Materials

1-Pentanol (≥99%), hexadecane (≥99%), poly(vinyl-pyrrolidone) (PVP K-30: Average M_w = 40,000 g mol^{-1}), Span 80 (sorbitan oleate), tetraehtyl orthosilicate TEOS (98%) and sodium citrate tribasic dihydrate (99%) were obtained from Sigma Aldrich. Ammonia (30%), hexane and ethanol were obtained from Fischer Scientific.

Synthesis of anisotropic rod shaped silica particles

To facilitate different rod diameters in as few batches as possible, two primary batches were synthesized (with d = 0.27 and 0.45 µm). These were then each split in half and one half was used to produce films whilst the other was used as seed particles in a coating reaction.

In a typical synthesis, initially stock solutions of PVP-K30 (100 g L^{-1}) in 1-pentanol and aqueous sodium citrate (0.18 M) were made up. PVP-K30 was dissolved in 1-pentanol by vigorous stirring ∼5 min and further sonication ∼30 min. Following this, sodium citrate (2.00 ml), de-ionised water (10.20 ml), ethanol (30.00 ml) and PVP-K30 in pentanol (300.00 ml) were added by syringe to a 500 ml laboratory bottle. This mixture was shaken vigorously by hand for approximately 30 seconds to generate a slightly turbid emulsion. After this, ammonia (5.00 ml for rods) was added by syringe and the bottle was again shaken for 30 s to encourage transport of ammonia into water droplets. TEOS (3.0 ml) was subsequently added to initiate growth. The reaction was then left for 24 hours and a subsequent aliquot of TEOS (3.0 ml) was added in some batches to promote further growth. Quantities used for the rods presented in this paper are given in Table 1. The mechanism of particle growth is thought to proceed by siliceous oligomers condensing together to form nuclei which migrate to the droplet interface and further condense. With additional growth, partial phase separation promotes the formation of a cap of silica with an attached water droplet that wets the growing interface only (see Figure 2 a). The final shape of the particle is dictated by interfacial tension and the degree of silica condensation.

To clean the particles, a round of centrifugation for 25 minutes at 4200g was performed and the supernatant was removed. Thereafter 3 more rounds of centrifugation were performed for a period of 5 minutes at 4200g re-dispersing the particles in ethanol each time. When required, in order to reduce the dispersity of the colloids,

G. Jacucci, B. W. Longbottom, C. C. Parkins, Prof. S. Vignolini

[a]Department of Chemistry, University of Cambridge, Lensfield Road, Cambridge CB2 1EW, UK

[#]e-mail: gi232@cam.ac.uk

B. W. Longbottom, C. C. Parkins, Prof. S. A. F. Bon

[b]Department of Chemistry, University of Warwick, Gibbet Hill Road, Coventry CV4 7AL, UK

selective centrifugation was then performed on the clean particles. This involved four rounds of centrifugation for 10 minutes at 117g (keeping solids) to remove smaller particles.

The reaction conditions used to obtain different rod diameters are displayed in Table 1.

TEOS / ml	NH_3 / ml	H_2O / ml	citrate / ml	EtOH / ml	r / µm	L / µm
3.00	5.00	9.50	2.00	30.00	0.135 ± 0.042	4.92 ± 0.79
0.50^a	3.60^a	5.00^a	-^{a}	150.00^a	0.171 ± 0.051	4.92 ± 0.79
$3.60 + 3.60^b$	6.00	12.24	2.4	36.0	0.225 ± 0.052	8.49 ± 2.44
0.83^c	6.00^c	8.30^c	-^{c}	250.00^c	0.25 ± 0.058	7.75 ± 2.1

Table 1: Comparison of reaction conditions in volume of reagents employed in the synthesis of a series of rod-shaped silica colloids with varying diameter. In all cases the amount of PVP in pentanol ($100\,\mathrm{g\,l^{-1}}$) was kept constant with respect to TEOS at a volume ratio of 100:1 pentanol:TEOS. Average radii and lengths are reported as measured manually from SEM images using ImageJ.[a]0.185 g of seed particles were used.[b]TEOS was added sequentially to promote further rod growth after allowing 6 h for the first portion to fully react.[c]0.304 g of seed particles used.

To investigate the phase space of possible aspect ratios, small batches of silica rods were synthesized (10 ml scale) with the following varying conditions (Table 2). These experiments were performed to find the optimal conditions for the synthesis of defined rod-shaped colloids with sufficiently high aspect ratio. A full discussion of the effect of each reagent on the particle dimensions was detailed by one of the authors.[?]

Series	Label	TEOS / ml	NH_3 / ml	H_2O / ml	citrate / ml	EtOH / ml
NH_3	a	0.10	0.30	0.20	0.10	1.00
	b	0.10	0.20	0.26	0.10	1.00
	c	0.10	0.10	0.32	0.10	1.00
	d	0.10	0.05	0.35	0.10	1.00
Citrate	e	0.10	0.17	0.23	0.11	1.00
	f	0.10	0.17	0.24	0.10	1.00
	g	0.10	0.17	0.25	0.09	1.00
	h	0.10	0.17	0.26	0.08	1.00
H_2O	i	0.10	0.18	0.30	0.08	1.00
	j	0.10	0.18	0.27	0.08	1.00
	k	0.10	0.18	0.25	0.08	1.00
	l	0.10	0.18	0.23	0.08	1.00
H_2O & Citrate	m	0.10	0.18	0.24	0.10 (0.18 M)	1.00
	n	0.10	0.18	0.20	0.10 (0.16 M)	1.00
	o	0.10	0.18	0.16	0.10 (0.14 M)	1.00
	p	0.10	0.18	0.12	0.10 (0.12 M)	1.00
EtOH	q	0.10	0.18	0.28	0.10	2.00
	r	0.10	0.18	0.28	0.10	1.50
	s	0.10	0.18	0.28	0.10	1.25
	t	0.10	0.18	0.28	0.10	1.00

Table 2: Comparison of reaction conditions in volume of reagents used to explore how different components affect particle morphology. In all cases the amount of PVP in pentanol ($100\,\mathrm{g\,l^{-1}}$) was kept constant with respect to TEOS at a volume ratio of 100:1 pentanol:TEOS.

Series	Label	$\chi_{\mathrm{TEOS}} : \chi_{\mathrm{NH_3}} : \chi_{\mathrm{H_2O}} : \chi_{\mathrm{citrate}}$	d / µm	L / µm	L/d
NH_3	a	1 : 12.11 : 47.21 : 0.027	0.218 (0.18)	3.46 (0.25)	15.87
	b	1 : 8.08 : 47.12 : 0.027	0.208 (0.20)	3.82 (0.36)	18.37
	c	1 : 4.04 : 47.03 : 0.027	0.203 (0.21)	6.17 (0.43)	30.39
	d	1 : 2.02 : 47.00 : 0.027	0.170 (0.31)	8.77 (0.29)	51.59
Citrate	e	1 : 6.66 : 41.67 : 0.044	0.200 (0.37)	7.86 (0.16)	39.30
	f	1 : 6.66 : 41.67 : 0.040	0.306 (0.36)	2.25 (0.22)	7.35
	g	1 : 6.66 : 43.48 : 0.036	0.294 (0.38)	2.07 (0.25)	7.04
	h	1 : 6.66 : 45.45 : 0.032	0.252 (0.31)	2.58 (0.19)	10.24
H_2O	i	1 : 7.14 : 55.55 : 0.032	0.225 (0.49)	1.39 (0.32)	6.18
	j	1 : 7.14 : 50.00 : 0.036	0.271 (0.32)	1.29 (0.1)	4.76
	k	1 : 7.14 : 45.45 : 0.040	0.280 (0.38)	1.06 (0.12)	3.79
	l	1 : 7.14 : 41.67 : 0.044	0.263 (0.30)	1.03 (0.18)	3.91
H_2O & Citrate	m	1 : 7.14 : 43.48 : 0.040	0.221 (0.31)	3.30 (0.13)	14.93
	n	1 : 7.14 : 38.46 : 0.036	0.310 (0.44)	1.16 (0.19)	3.74
	o	1 : 7.14 : 33.33 : 0.031	0.131 (0.29)	3.88 (0.26)	29.62
	p	1 : 7.14 : 28.57 : 0.027	0.260 (0.64)	2.34 (0.37)	9.00
EtOH	q	1 : 7.14 : 47.61 : 0.027	0.103 (0.36)	3.92 (0.43)	36.98
	r	1 : 7.14 : 47.61 : 0.027	0.241 (0.28)	1.39 (0.25)	5.77
	s	1 : 7.14 : 47.61 : 0.027	0.382 (0.27)	1.04 (0.14)	2.72
	t	1 : 7.14 : 47.61 : 0.027	0.326 (0.39)	0.72 (0.18)	2.21

Table 3: Comparison of reaction conditions in molar ratios of tetraethyl ortho silicate : ammonia : water : trisodium citrate dihydrate and resulting average particle diameters, d, and length, L, both with dispersity given in parenthesis calculated from standard deviation over the average diameter $\rho = \sigma/d$ as shown in Figure 1

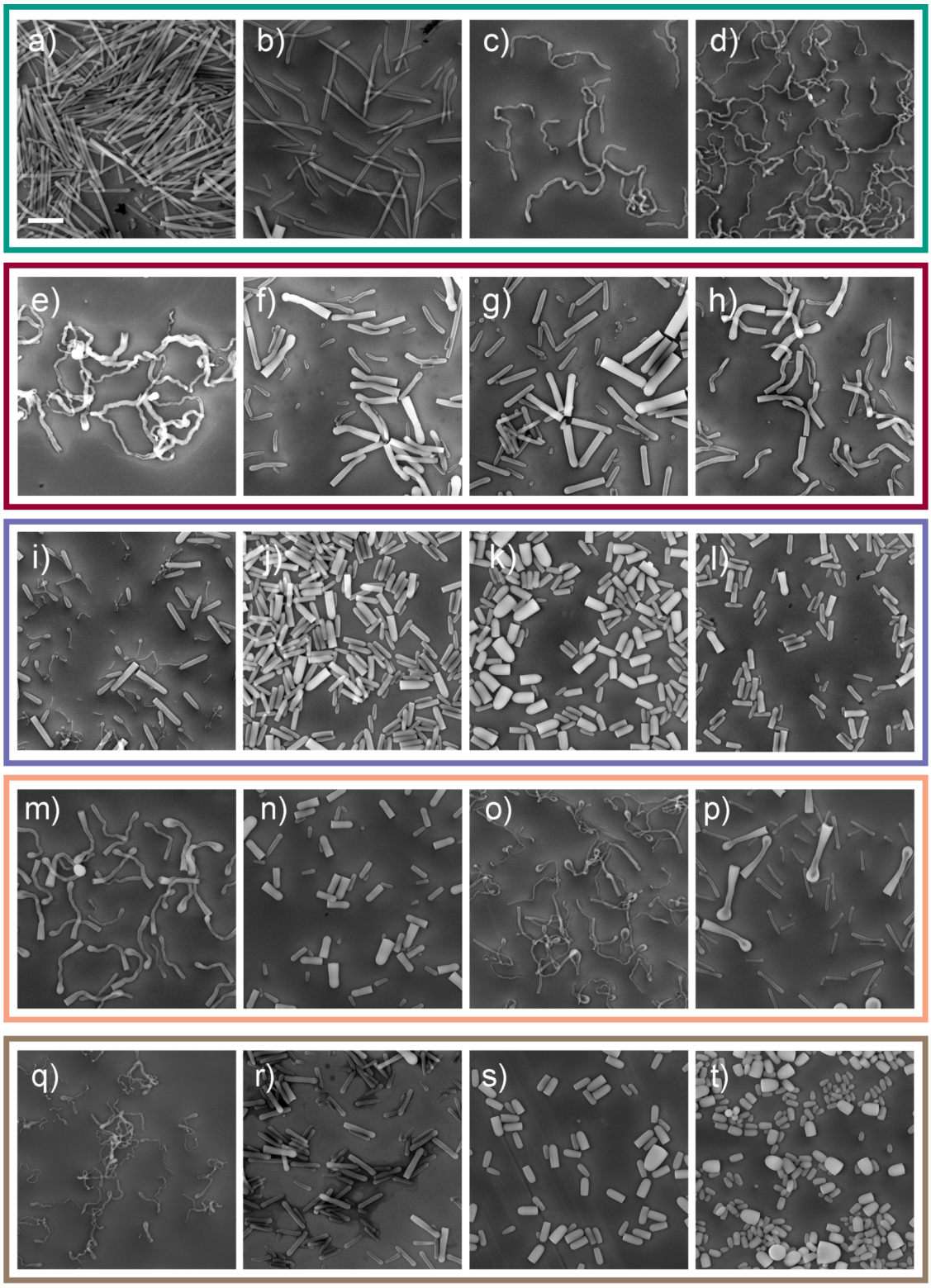

Figure 1: Scanning Electron Microscopy (SEM) images of anisotropic silica particles produced by varying [NH_3]: χ_{NH_3} = 12, 8, 4 and 2 for (a–d cyan), [citrate]: $\chi_{citrate}$ = 4.4, 4, 3.6 and 3.2×10^{-2} for (e–h red), [H_2O]: χ_{H_2O} = 55, 50, 45, 42 for (i–l blue), [citrate] and [H_2O] simultaneously (m–p orange) and [EtOH]: vol = 2, 1.5, 1.25 and 1 ml for (q–t brown). Reagent concentrations decrease reading left to right with amounts detailed in Table 3. Scale bar = $2\,\mu m$.

Synthesis of isotropic spherical silica particles

In order to synthesize spherical silica colloids of comparable dimensions to the above rod-shaped particles, a standard Stöber synthesis was deployed. Briefly, TEOS was mixed with ethanol in a 250 ml RBF by stirring with a magnetic stir bar (∼500 rpm) and to this ammonia was added to catalyze the hydrolysis-condensation reaction. The reaction was performed at room temperature (∼20 °C) and left overnight to ensure full conversion. Particles were cleaned by 3 successive rounds of centrifugation, redispersing in ethanol each time.

The reaction conditions used to obtain different particle diameters are displayed in Table 4.

TEOS / ml	NH_3 / ml	EtOH / ml	r_{SEM} / µm	r_{DLS} / µm
6.0	12.5	150.0	0.113 ± 0.016	0.128 ± 0.022
6.0	25.0	150.0	0.172 ± 0.006	0.200 ± 0.006
6.0	50.0	150.0	0.224 ± 0.006	0.251 ± 0.006
6.0	60.0	150.0	0.279 ± 0.007	0.267 ± 0.005

Table 4: Comparison of reaction conditions in volume of reagents employed in the synthesis of a series of spherical silica colloids with varying diameter. Average radii for r_{SEM} are reported as measured manually from SEM images using ImageJ. Uncertainty is reported as the standard deviation.

Preparation of colloidal films

Prior to preparing films of targeted thickness, silica particles were dried in a vacuum oven at 60 °C. The dried particles were then dispersed in water to make up known volume fractions (using a measured absolute density, $\rho = 2.16\,\mathrm{g\,cm^{-3}}$): $\phi_{Disp.} = 0.1$, 0.05, 0.025, 0.0125 and 0.00625 of which 100 µl of each were deposited (immediately after vortexing the dispersions) onto glass microscope slides with an adhesive spacer (9 × 9 mm Frame-Seal Bio-Rad) by simple drop-casting (Figure 2 b) under ambient conditions, $T = 20\,°\mathrm{C}$. These slides were then contained within petri dishes to enable a steady state of humidity during the drying process.

The volume/packing fraction of the dried films were estimated from the ratio of the volume of added solids over the measured volume of the film: $\phi_{\mathrm{Film}} = V_{\mathrm{solids}}/V_{\mathrm{film}} = (V \times \phi_{\mathrm{Disp.}})/(\mathrm{Area} \times \mathrm{Height})$. Where V is the volume of dispersion dropped - 100 µl, and the height was taken as the average film thickness.

rods		**spheres**	
r / µm	FF	r / µm	FF
0.135 ± 0.042	0.53	0.113 ± 0.016	0.58
0.171 ± 0.051	0.52	0.172 ± 0.006	0.51
0.225 ± 0.052	0.56	0.224 ± 0.006	0.63
0.25 ± 0.058	0.62	0.279 ± 0.007	0.59

Table 5: Comparison of the average calculated filling fractions, FF (ϕ_{Film}), for the series of films for each size of colloid for both rods and spheres. Overall the average FF was high and similar for films constructed of either rod-shaped or spherical colloids.

Note on uncertainties in film filling fraction

As film filling fraction is an important parameter in quantifying the transport mean free path (see Equation 4), we briefly discuss here the sources of error in its determination.

The systematic errors introduced by weighing and pipetting in the preparation of the films are relatively small. For example if we take the expected worst-case scenario i.e. a thin film prepared from a serially diluted stock colloid suspension:

1. 100 ± 0.1 mg Silica Rods (density $2.16\,\mathrm{g\,cm^{-3}}$ measured by pycnometry) was dispersed in 416 ± 1 µl H_2O to prepare a stock colloid volume fraction of 0.1 ± 5.3e-4.
2. The stock was serially diluted 4 times by half each time to reach a volume fraction of 6.25e-3 ± 3.25e-5.
3. 100 ± 0.1 µl colloid dispersion was pipetted onto a clean glass slide with an adhesive 9 × 9 mm gasket.
4. The sample was incubated in a small petri dish to maintain a steady state of humidity during drying.
5. Film thickness was measured using both interferometry and cross-sectional SEM and found to be in good agreement with ∼2-5% uncertainty from the standard deviation = 12.36 ± 0.66 µm.
6. FF = (1e-7 [±1e-10]*6.25e-3 [±3.25e-5])/(0.009 [±1e-4]^2*12.36e-6 [±0.66e-6]) = 0.62 ± 0.04.

The relatively wide range of calculated filling fractions of prepared films noted in Table 5 is therefore a product of small changes in drying conditions i.e. temperature and humidity.

Preparation of supracolloidal balls

Silica rods were assembled into supracolloidal balls by a simple solvent emulsion-evaporation method (Figure 2 c). Briefly, 100 µl of silica rod aqueous dispersion ($\phi = 0.1$) was added to 200 µl of span 80 in hexadecane (2 wt.%) in a 1.5 ml eppendorf tube. For disordered balls, the aqueous phase was prepared with 0.01 M of calcium chloride. The mixture was vortexed for approximately 10 seconds to form a water-in-oil emulsion with the colloids confined to the aqueous phase. This emulsion was then poured out into a petri dish containing 2 ml of span 80 (0.5 wt.% in hexadecane). Evaporation of the water phase took approximately 48 h. The speed of evaporation could be increased by reducing the the volume of hexadecane in the petri dish. The supracolloidal balls were then collected with a plastic pipette from the bottom of the petri dish and were cleaned by redispersing in hexane. This was performed 3 times, allowing the balls to sediment to the bottom of the vial/eppendorf, in order to remove excess surfactant.

Material characterization

Samples for SEM imaging for the reaction condition series were prepared by diluting the particle solutions to around $0.5\,\mathrm{mg\,ml^{-1}}$ in ethanol and allowing them to dry onto silicon wafers supported on aluminium stubs with a conductive copper adhesive. SEM imaging of particles was performed on a Zeiss Gemini SEM 500 or TESCAN MIRA3 FEG-SEM at 10 kV. Particle films were imaged directly on the glass microscope slides by fracturing the slides to reasonable dimensions for SEM imaging and supporting them with copper adhesive on 45° aluminium stubs. A long working distance of 8 mm was deployed with an accelerating voltage of 2 kV using the secondary electron detector (SE2) to collect images in order to avoid charging effects.

The absolute (skeletal) density of the silica rods helium pycnometry was measured on dried powder samples using a Micro-meritics Accupyc 1330 Helium Pycnometer.

Film thicknesses were determined by using a Bruker Contour GT-X interferometer with a 5× objective and via cross-sectional SEM imaging of a fractured film. For interferometry, 10 × 10 mm sections were measured by stitching with 20% area overlap. The glass slide that samples were deposited on served both as a reference for height = 0 and was useful as a flat reflective surface to align the stage. For SEM imaging, stage tilt angles of 40° were used along with a 45° mounting stub to total 85° of tilt. A correction was applied for the small difference from a perpendicular view using $T_{corr} = T_{app} \times \sin(45 + t) \times \frac{\pi}{180}$, where T_{corr} = corrected thickness, T_{app} = apparent thickness and t = stage tilt angle.

Optical characterization

The transport mean free path (ℓ_t) of the silica films was determined using total transmission measurements. A light source (Ocean Optics HPX-2000) was coupled into an optical fiber (Thorlabs FC-UV100-2-SR) via a collimator (Thorlabs). The transmitted light was collected with an integrating sphere (Labsphere) and the signal was acquired by a spectrometer (Avantes HS2048). The signal was normalized with respect to the intensity when no sample was mounted.

The optical properties of single silica supraparticles were characterized on a Zeiss Axio Scope A1 microscope using a halogen lamp (Zeiss HAL100) as a light source in Koehler illumination in a reflection geometry. The reflected intensity was acquired using a 100x objective (Zeiss, LD EC Epiplan-Neofluar, 100x, NA 0.95) and

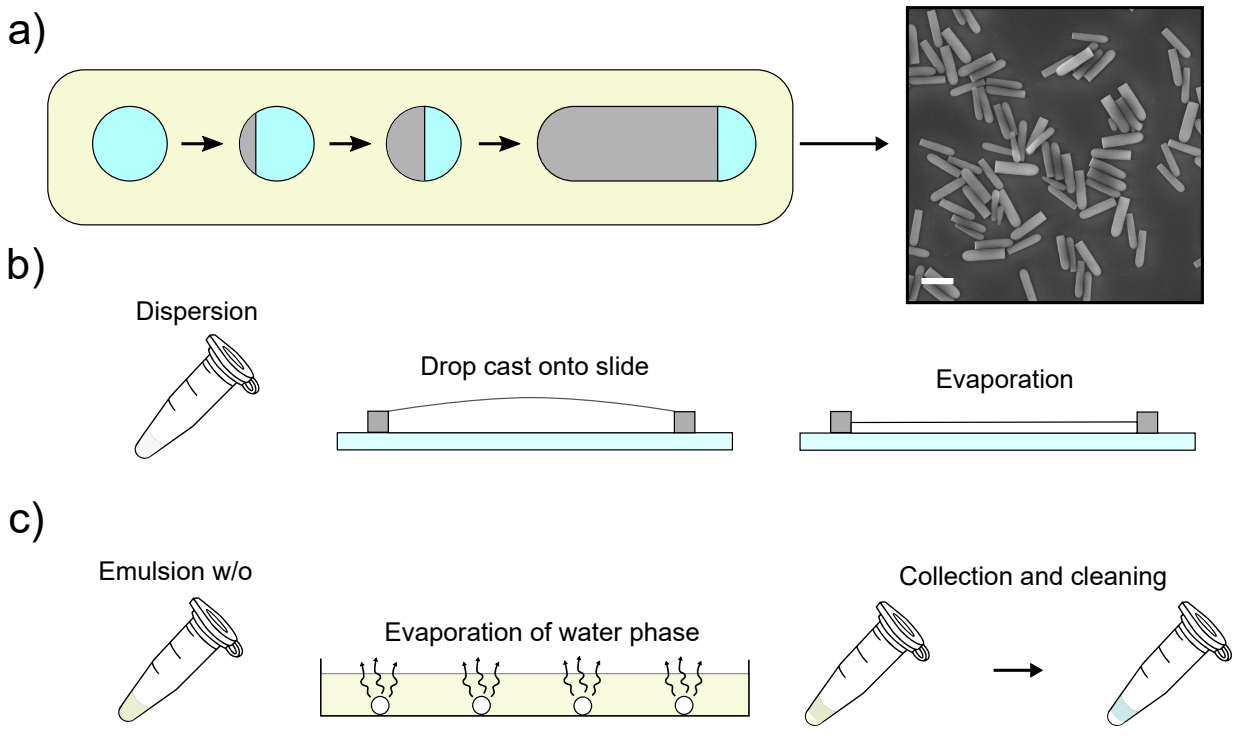

Figure 2: General fabrication scheme for colloidal silica rods a), assembly into films by drop casting b) and assembly under confinement into supracolloidal balls c).

a spectrometer coupled (Avantes HS2048) to an optical fibre (Avantes, FCUV50-2-SR, 50 μm core size). The reflectance spectra were acquired in bright field and normalized against a silver mirror (PF05-03-P01, Thorlabs).

Quantifying the transport mean free path

In Figure 1 of the main text we presented the transport mean free path for silica films made of colloids with different anisotropies. The total transmitted data where fitted using the following formula, which is the solution of the diffusion equation in a slab geometry:[?,?]

$$T = \frac{2z_e\ell_t}{L + 2z_e\ell_t}, \tag{1}$$

where L is the slab thickness, T is the total transmission and z_e is the extrapolation length.

The extrapolation length was estimated from the following equation:

$$z_e = \frac{2}{3}\frac{1+R}{1-R} \tag{2}$$

where R is the angle- and polarisation-averaged reflection coefficient at the slab interface.

R can be obtained by:[?]

$$R = \frac{3\int_{-\pi/2}^{0} R(\theta)sin(\theta)cos^2(\theta)d\theta + 2\int_{0}^{\pi/2} R(\theta)sin(\theta)cos(\theta)d\theta}{3\int_{-\pi/2}^{0} R(\theta)sin(\theta)cos^2(\theta)d\theta - 2\int_{0}^{\pi/2} R(\theta)sin(\theta)cos(\theta)d\theta + 2} \tag{3}$$

where $R(\theta)$ is the polarization averaged reflection coefficient obtained from Fresnel's equations.[?]

To calculate R, the effective refractive index (n_e) of the silica network was estimated by the Maxwell-Garnett's theory:[?]

$$n_e = \frac{1 + 2ff(\frac{n^2-1}{n^2+2})}{1 - ff(\frac{n^2-1}{n^2+2})} \tag{4}$$

where ff and n are the filling fraction and the refractive index of silica, respectively. In this work, n_e and consequently z_e were calculated starting from an experimental estimate of the filling fraction (see section section for calculation).

Numerical simulations of the optical properties

The scattering properties of ensembles of isotropic particles with different size distributions were investigated using a numerical approach to generate two-dimensional systems with a controlled morphology.[?] The optical properties of these systems were then computed using LUMERICAL 8.22 (Lumerical Solutions Inc., Vancouver, BC, Canada), a commercial-grade software using the finite-difference time-domain (FDTD) method. The value of mean free path reported in Figure 4 were calculated from the simualated spectra and using Equation 1.

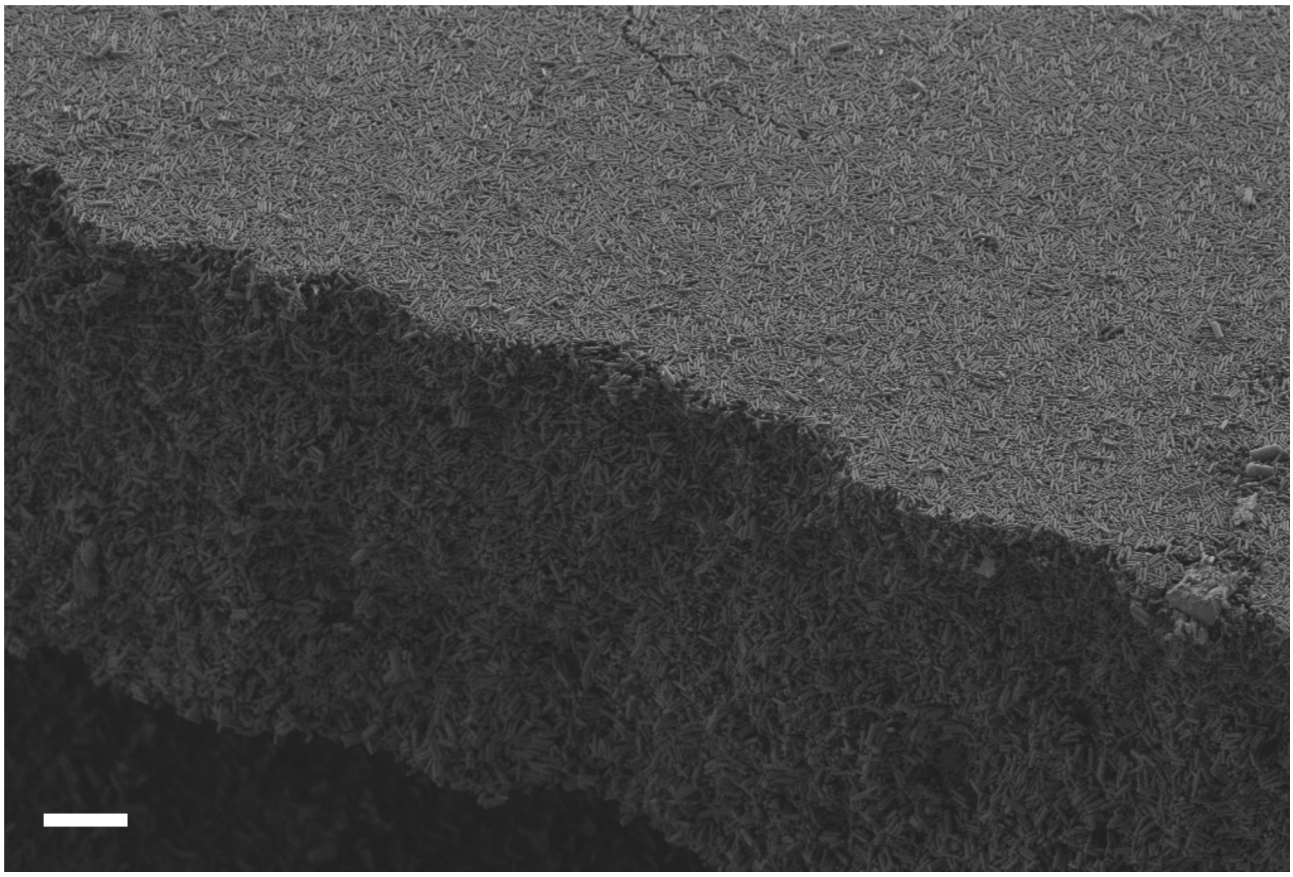

Figure 3: Low magnification SEM cross-section of film assembled from silica rods. Scale bar $= 10\ \mu\mathrm{m}$

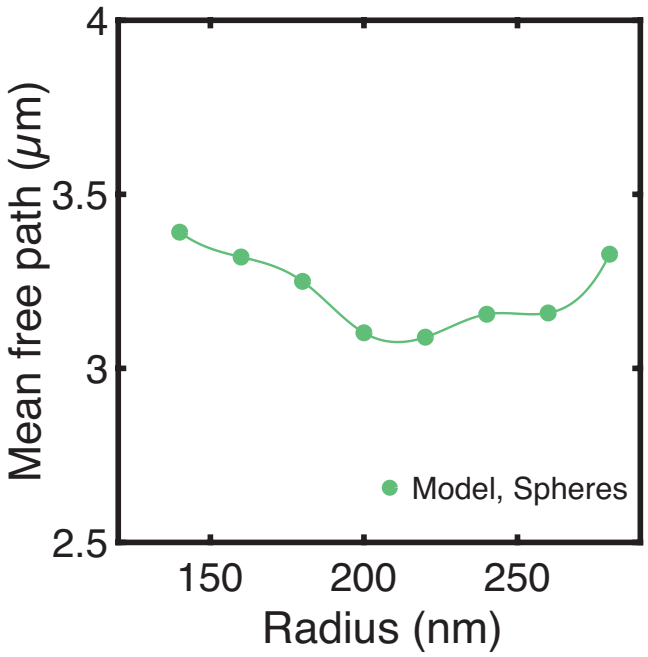

Figure 4: Numerical simulations of the optical properties of silica-based systems. The theoretical minimum of the mean free path is in good agreement with what experimentally observed (r=225nm in Figure 1d of the main text). All simulated systems have a thickness of 5 μm, a filling fraction of ff=0.5.

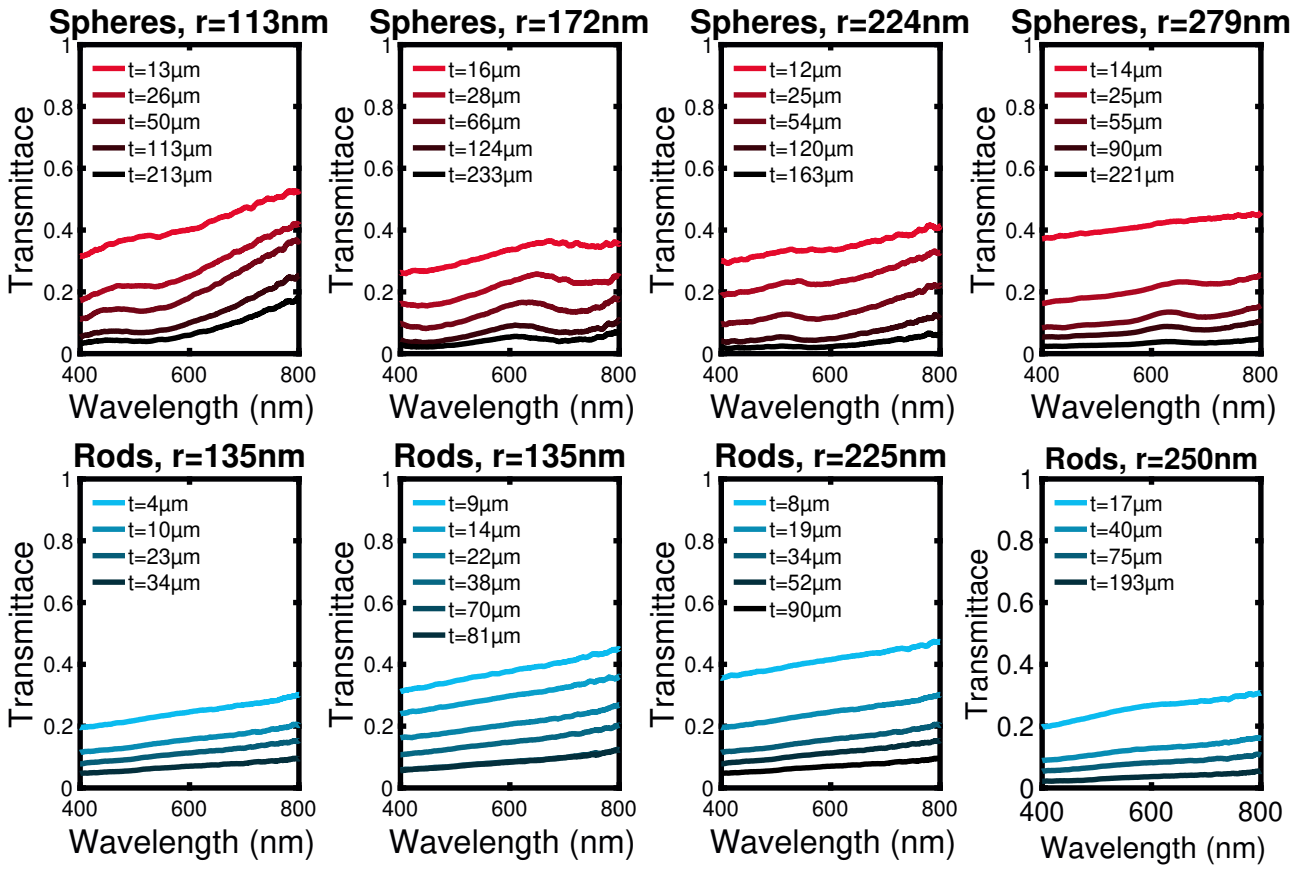

Figure 5: Wavelength dependency of the total transmittance. Assemblies of rod-shaped colloids (cyan) show a less marked dependency on the wavelength than systems made of spherical colloids (red).

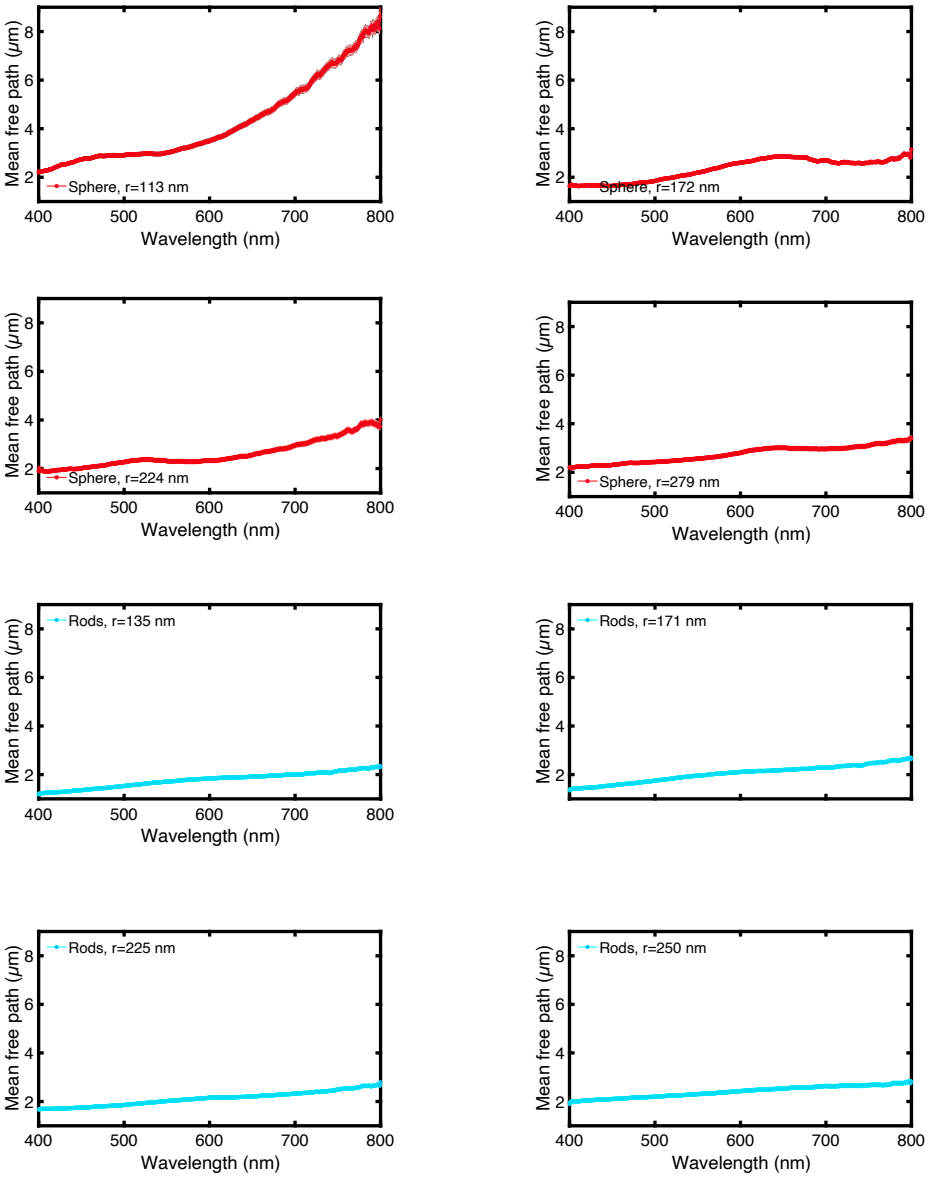

Figure 6: Wavelength dependency of the transport mean free. Assemblies of rod-shaped colloids (cyan) show a less marked dependency on the wavelength than systems made of spherical colloids (red).

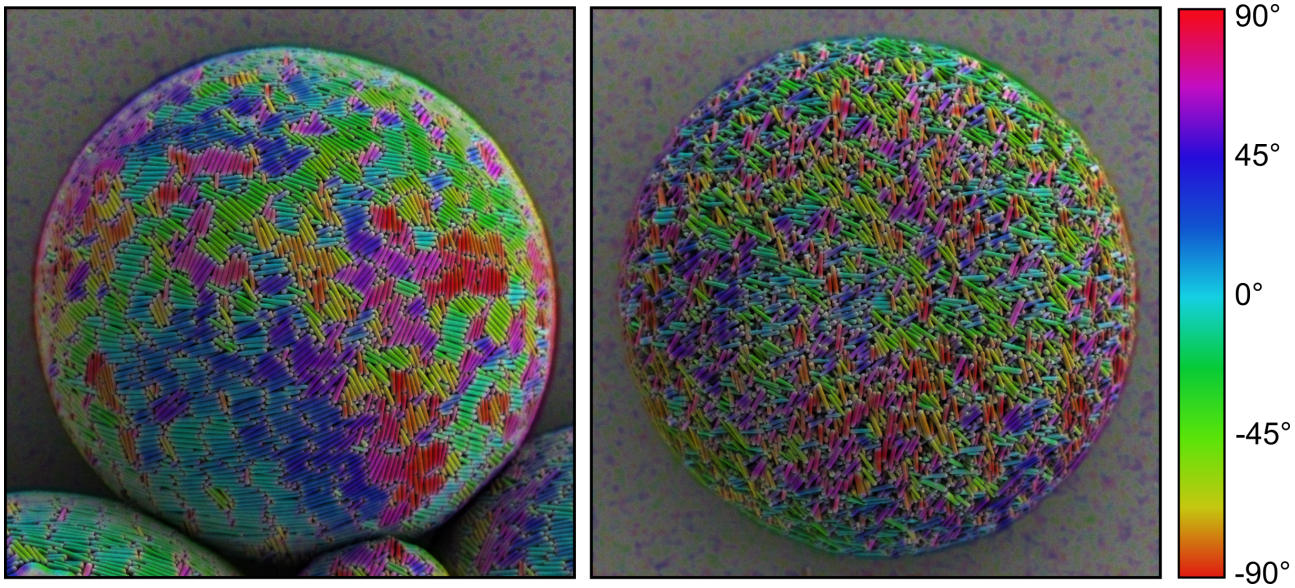

Figure 7: Visualization of rod orientation in supracolloidal balls by colour mapping. Ordering at the surface is highlighted on the supracolloidal ball on the left whereas it is absent from supracolloidal ball on the right assembled in the presence of $CaCl_2$. Analysis was done in imageJ using the OrientationJ plugin, cubic spline method with $\sigma = 2$.

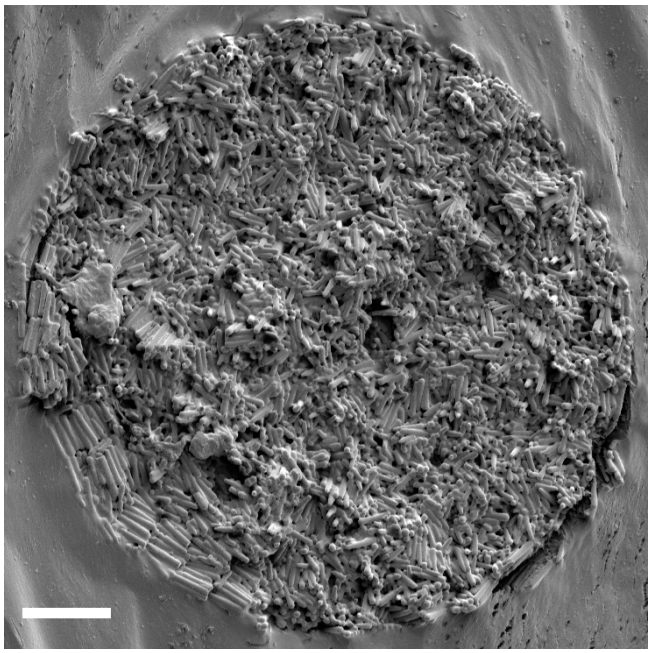

Figure 8: SEM image of the cross section of a supracolloidal ball. Some ordering of rods can be seen near the outer layers (most obvious in the lower left of the image) but this does not appear to propagate through to the centre of the particle. The sample was prepared by embedding the particles in nail varnish and subsequently freeze fracturing upon submerging in liquid nitrogen. Scale bar $= 5\,\mu\mathrm{m}$.

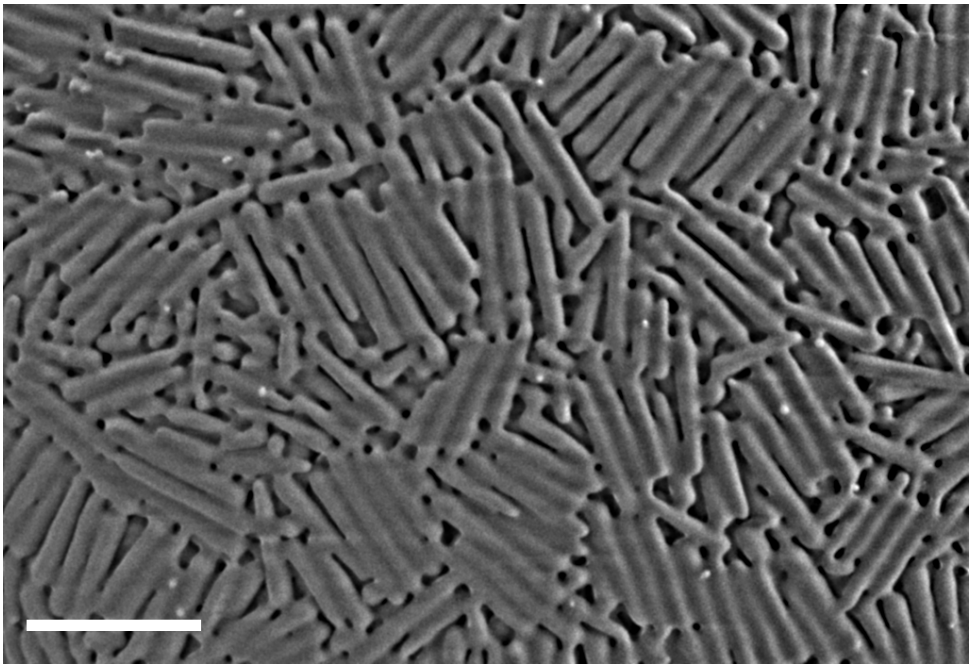

Figure 9: SEM image of the surface of a sintered supracoilloidal ball. Rods were fused where contacts were made. Scale bar $= 2\,\mu\mathrm{m}$.

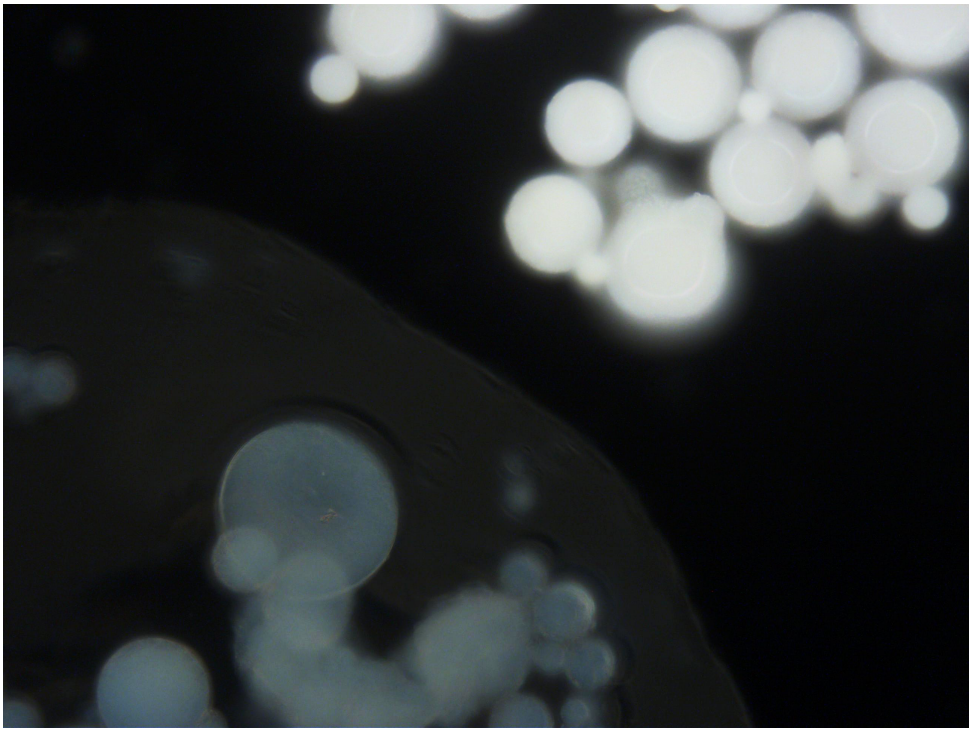

Figure 10: Micrograph of sintered supraparticles imaged in dark field. The supraparticles in the lower left were immersed in water whilst those in the top right were in air (interface just visible as faint line).When wet, the supraparticles turn transparent and do not disintegrate (microstructure is preserved).

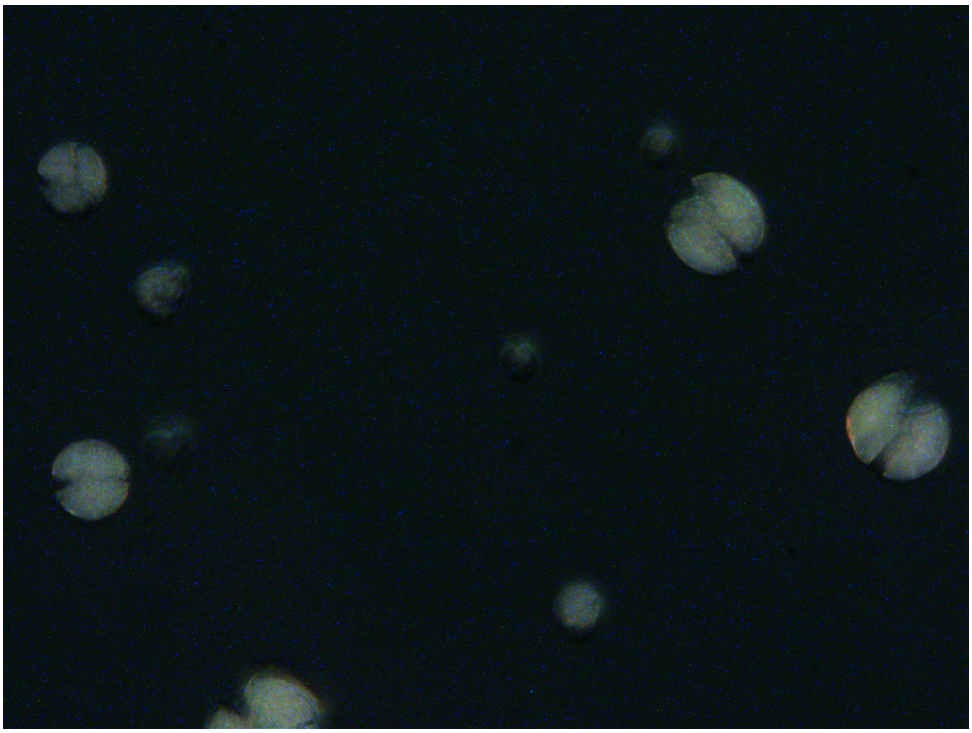

Figure 11: Micrograph of non-sintered supraparticles imaged in dark field. Uppon wetting, the supraparticles disintegrate (microstructure is not preserved).